

MODELLING ELECTROLYTE AND WATER TRANSPORT IN THE KIDNEY OF A PREGNANT RAT: EFFECTS OF TRANSPORT INHIBITORS

MELISSA STADT^{*} AND ANITA T. LAYTON[†]

^{*} Department of Applied Mathematics, University of Waterloo, Waterloo, Ontario, Canada
e-mail: mstadt@uwaterloo.ca

[†] Departments of Applied Mathematics and Biology, Cheriton School of Computer Science, and
School of Pharmacy, University of Waterloo, Waterloo, Ontario, Canada
email: anita.layton@uwaterloo.ca

Key words: Kidney Physiology, Pregnancy, Computational Model, Epithelial Transport, Natriuresis.

Abstract. During pregnancy, major adaptations in renal morphology, hemodynamics, and transport occur to achieve the volume and electrolyte retention required in pregnancy. These complex changes can appear counterintuitive when considered in isolation. Additionally, in pregnancies complicated by a disorder, such as gestational hypertension, kidney function may be altered from normal pregnancy. To analyze how renal function is altered during pregnancy, we developed epithelial cell-based computational models of solute and water transport in a nephron of the kidney for a rat in mid- and late-pregnancy. The model represents known pregnancy-induced changes in renal transporters, including reduction in proximal tubule and medullary loop transporters. The pregnant rat nephron models predicted urine output and excretion consistent with measured values. Additionally, we simulated the inhibition and knockout of the ENaC and H⁺-K⁺-ATPase transporters. Our simulations predicted that ENaC and H⁺-K⁺-ATPase transporters are essential for sufficient Na⁺ and K⁺ reabsorption during pregnancy.

1 INTRODUCTION

During pregnancy, the plasma volume of the mother must expand drastically to support the rapidly developing fetus and placenta [1]. Normally, in a virgin or non-pregnant state, the kidneys excrete almost all Na⁺ intake through urine, but in pregnancy this is not the case: there is net Na⁺ retention in a pregnant rat depending on sufficient dietary intake. Additionally, in late pregnancy, maternal net K⁺ retention occurs [2]. These changes are supported by major adaptations in kidney function, including markedly elevated glomerular filtration to the kidneys, increased kidney size and length of the proximal tubule, and both increased and decreased membrane transporter activities along the various nephron segments [3-7].

In this study, we developed computational models of a nephron in a pregnant rat kidney to investigate the impact of key pregnancy-induced renal adaptations on Na⁺ and K⁺ handling *in silico*. We built two computational models: one that represents kidney function at mid-pregnancy and another that represents kidney function at late pregnancy. The female-specific rat kidney model developed by Hu et al. [8] is used as a virgin control in this study. Two pregnancy models were necessary because of the drastically changing demands of a growing fetus and placenta through a pregnancy. Using these models we investigate the impact of key

pregnancy-induced renal adaptations on Na^+ and K^+ handling in the kidney. Additionally, we consider the impact of epithelial Na^+ channel and H^+-K^+ -ATPase knockout and inhibition on kidney Na^+ and K^+ transport during pregnancy based on published experimental studies (see Refs. [9, 10]).

2 MATERIAL AND METHODS

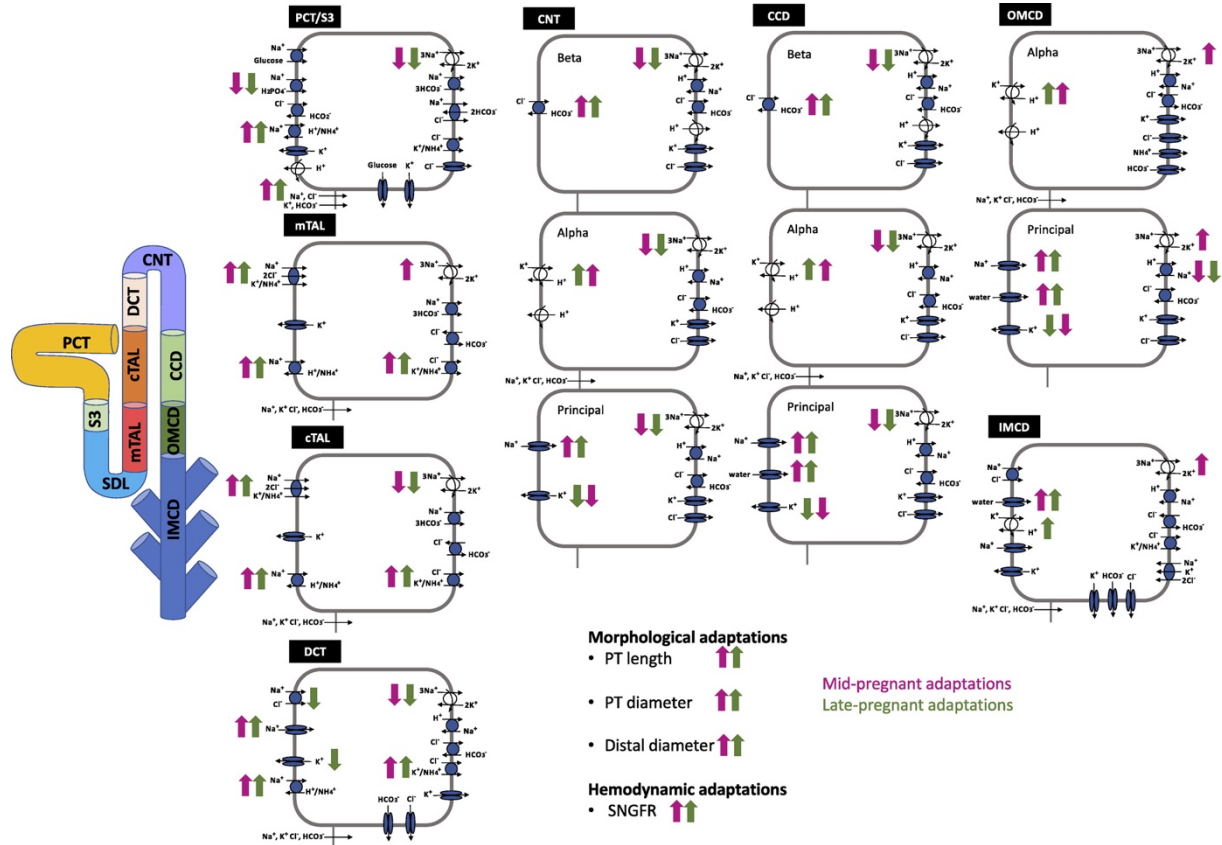


FIGURE 1. Schematic diagram of superficial nephron cells with pregnancy adaptations. The diagram displays main Na^+ , K^+ , and Cl^- transporters as well as aquaporin water channels. Midpregnant adaptations from nonpregnancy are indicated by pink arrows. Late-pregnant adaptations from nonpregnancy are indicated by green arrows. Upward orientation indicates an increase; downward orientation indicates a decrease. No arrow indicates that the transporter is not changed in the respective model. CCD, cortical collecting duct; cTAL, cortical thick ascending limb; CNT, connecting tubule; DCT, distal convoluted tubule; IMCD, inner medullary collecting duct; mTAL, medullary thick ascending limb; OMCD, outer medullary collecting duct; PCT, proximal convoluted tubule; PT, proximal tubule; SDL, short descending limb; SNGFR, single-nephron glomerular filtration rate; S3, proximal straight tubule. Reprinted from Ref. [11] with permission.

Our group have published a series of epithelial cell-based models of kidney function in the male rat [12-19], female rat [8, 20, 21], and human [21-23]. The female rat kidney model [20] was used as a control in this study and referred to as the NP (non-pregnant) model. In this study, we extended the NP model to simulate solute and volume transport along a superficial nephron of (1) a mid-pregnant (MP) kidney and (2) a late-pregnant (LP) rat kidney. Note that normal rat gestation is approximately 21–22 days [24]. The MP rat model represents nephron

transport at ~12–15 days of gestation (i.e., about halfway through gestation). The LP rat model represents nephron transport at ~19–20 days of gestation (i.e., near the end of rat gestation). As previously noted, we built separate models for MP and LP because there are distinct adaptations during the different stages of pregnancy due to the growing demands of the developing fetus and placenta. Because the original model equations in the study by Hu et al. [20] were based on mass conservation that is similarly valid in pregnancy, those same equations were used here, but appropriate parameter values were changed to account for renal adaptations during MP and LP. These parameter changes can be found in Table 1 of Ref. [11].

The cell-based epithelial transport model represents functionally distinct segments as follows: the PCT, proximal straight tubule (also known as the S3 segment), short descending limb, thick ascending limb divided into the medullary and cortical segments, distal convoluted tubule, connecting tubule, and collecting duct divided into the cortical, outer- and inner-medullary segments. Each nephron segment other than the proximal tubule (which is compliant, as discussed in the following section) is represented as a rigid tubule lined by a layer of epithelial cells, with apical and basolateral transporters that vary according to cell type. Each nephron segment has distinct transporters, permeabilities, and morphological properties. The model accounts for the following 15 solutes: Na^+ , K^+ , Cl^- , HCO_3^- , H_2CO_3 , CO_2 , NH_3 , NH_4^+ , HPO_4^{2-} , H_2PO_4^- , H^+ , HCO_2^- , H_2CO_2 , urea, and glucose. The model is a large system of coupled ordinary differential and algebraic equations, solved for steady state, and predicts luminal fluid flow, hydrostatic pressure, luminal fluid solute concentrations, cytosolic solute concentrations, membrane potential, and transcellular and paracellular fluxes. A schematic diagram of the model, with MP and LP changes highlighted, is shown in Fig. 1.

2.1 Pregnancy-specific models

We created pregnancy-specific models (i.e., MP and LP) by increasing or decreasing relevant NP model parameter values based on experimental findings in the literature [11]. The first major change in the MP and LP models is the increase in single-nephron glomerular filtration rate (SNGFR). MP and LP SNGFR were increased by 30% and 20%, respectively, from the NP SNGFR value. These increases were based on findings in the study by Baylis [25], where euvoletic pregnant rats were studied. Specifically, MP and LP SNGFR values were 31 and 29 nL/min, respectively, versus 24 nL/min in NP. The elevated SNGFR significantly increases the filtered load at the beginning of the nephron in both MP and LP models. In addition, during pregnancy, plasma osmolality is decreased, where plasma Na^+ concentration and Cl^- concentration slightly decreased, but with slightly elevated plasma K^+ concentration in LP [5, 26]. These changes are small compared with the SNGFR increases; thus, filtered loads are still substantially elevated.

During pregnancy, kidney volume increases [27, 28]. In particular, it has been shown that the proximal tubule lengthens [28]. Accordingly, we increased the proximal tubule length by 14% and 17% in MP and LP models, respectively. Based on the increased kidney volume and the observed dilation in the collecting system during pregnancy [29], we assumed that the diameter increased by 7% in the proximal tubule and 5% in downstream segments in both pregnant rat models. Although tubular diameter has not been measured experimentally, without assuming this small tubular dilation, the much-elevated volume flow in pregnancy would cause an excessive drop in tubular fluid pressure.

3 RESULTS

3.1 Baseline results

Model simulations were conducted for the NP, MP, and LP models to determine how pregnancy-induced changes in renal hemodynamics, morphology, and transporter activity together modify tubular transport in the superficial nephrons of the rat kidney. Predicted tubular flows key solutes and water along the model nephron are shown in Fig. 2. Segmental solute and water transport is displayed in Fig. 3.

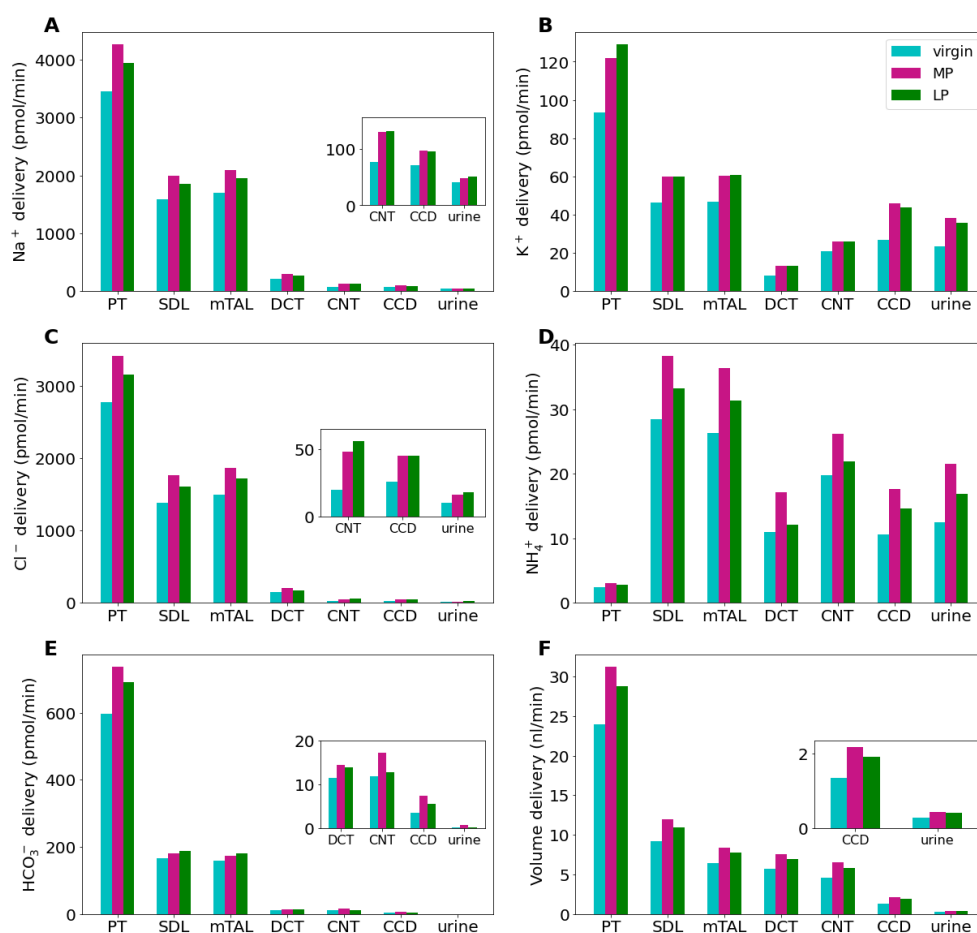


FIGURE 2. Delivery of key solutes (A–E) and volume (F) to the beginning of the individual nephron segments in the nonpregnant, mid pregnant (MP), and late pregnant (LP) models. Rightmost bars are urinary excretions. *Insets*: reproduction of distal segment values. CCD, cortical collecting duct; CNT, connecting tubule; DCT, distal convoluted tubule; mTAL, medullary thick ascending limb; PT, proximal tubule; SDL, short descending limb.

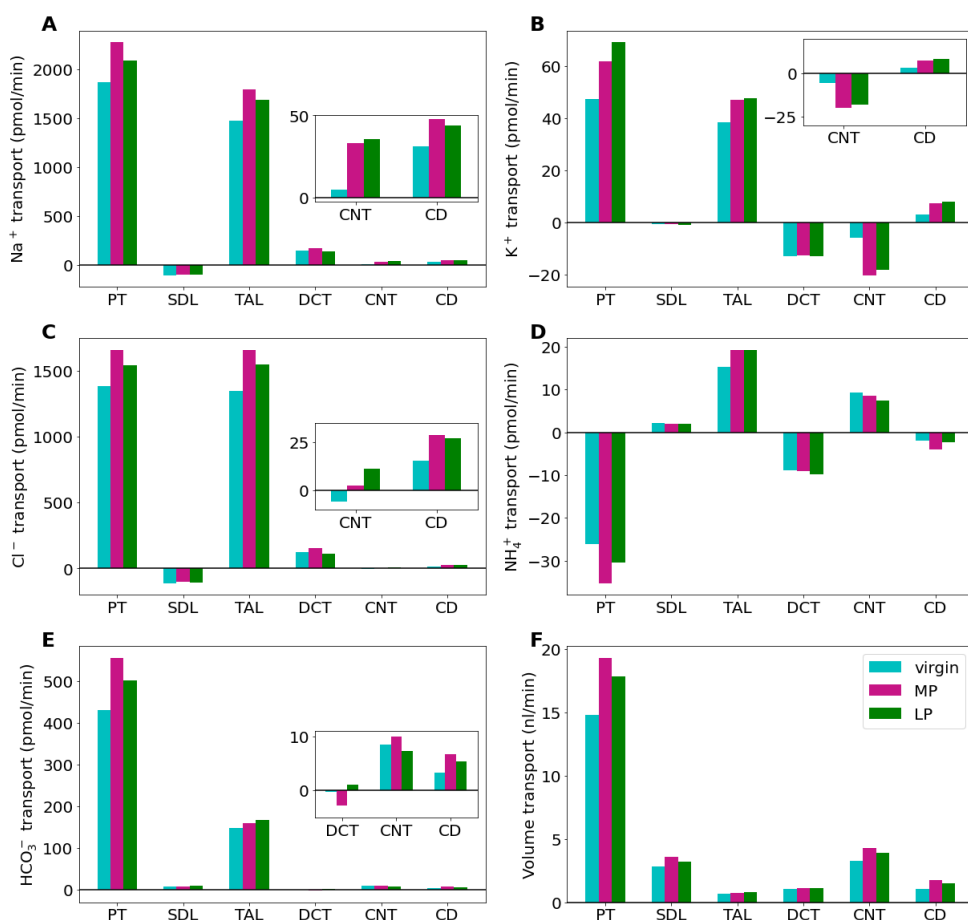


FIGURE 3. Net segmental transport of key solutes (A–E) and volume (F) along the individual nephron segments in the non-pregnant, mid-pregnant, and late-pregnant models. Transport is positive out of the nephron segment, i.e., positive transport shows net reabsorption and negative net secretion along that segment. Notations are analogous to Fig. 2.

In the NP model, 58% of the filtered Na⁺ is reabsorbed along the proximal tubule, primarily via the coordinated transport of apical Na⁺-H⁺ exchanger 3 (NHE3) and basolateral Na⁺-K⁺-ATPase. In MP and LP, the pregnancy-induced hyperfiltration, tubular hypertrophy, and elevated NHE3 activity increase net Na⁺ reabsorption along the proximal tubule by 27% and 18%, respectively (Fig. 3). Most of the remaining Na⁺ is reabsorbed downstream along the thick ascending limb. Due to the enhanced Na⁺-K⁺-Cl⁻ cotransporter 2 (NKCC2) and NHE activity, Na⁺ transport along the thick ascending limbs is predicted to be ~18% and 8% higher in the MP and LP models, respectively. Na⁺ reabsorption is similar in each of the NP, MP, and LP models. Urine Na⁺ excretion is 32, 34, and 35 pmol/min for the NP, MP, and LP models, respectively. Urinary Na⁺ excretion is the highest in LP, at 10% above the NP model (Fig. 2).

The model predicts that 54% of filtered K⁺ is reabsorbed along the proximal tubule of the NP model. Net K⁺ reabsorption along the proximal tubule increases by 36% in MP and 52% in LP (Fig. 3). Like Na⁺, most of the remaining K⁺ is also reabsorbed along the thick

ascending limb. Downstream of the loop of Henle, the distal convoluted tubule and connecting tubule vigorously secrete K^+ (Fig. 3). In MP, K^+ secretion along these distal segments is decreased by 10% despite increased epithelial Na^+ channel (ENaC) activity that would, in isolation, increase K^+ secretion. In addition, reabsorption in the collecting duct is increased by 54% compared with the NP model. Similar changes occur in LP. These changes lead to 29% and 42% more accumulated K^+ reabsorption along the full nephron during MP and LP, respectively (Fig. 3).

The majority (65%) of the filtered volume is reabsorbed along the proximal tubule in the NP model (Fig. 2). Water reabsorption along the proximal tubule, which follows Na^+ transport, increases by 34% and 25% in MP and LP, respectively (Fig. 3). This yields a similar fractional reabsorption of $\sim 68\%$ in both MP and LP models along the proximal tubule. More water is reabsorbed downstream, albeit at a slower rate. The models predict a urine output of 0.25 nL/min/nephron (superficial) in the NP model and ~ 0.30 nL/min/nephron (superficial) in both MP and LP models. The increase in volume excretion during pregnancy is within reported ranges [5, 28].

3.2 Effect of ENaC inhibition on Na^+ and K^+ transport

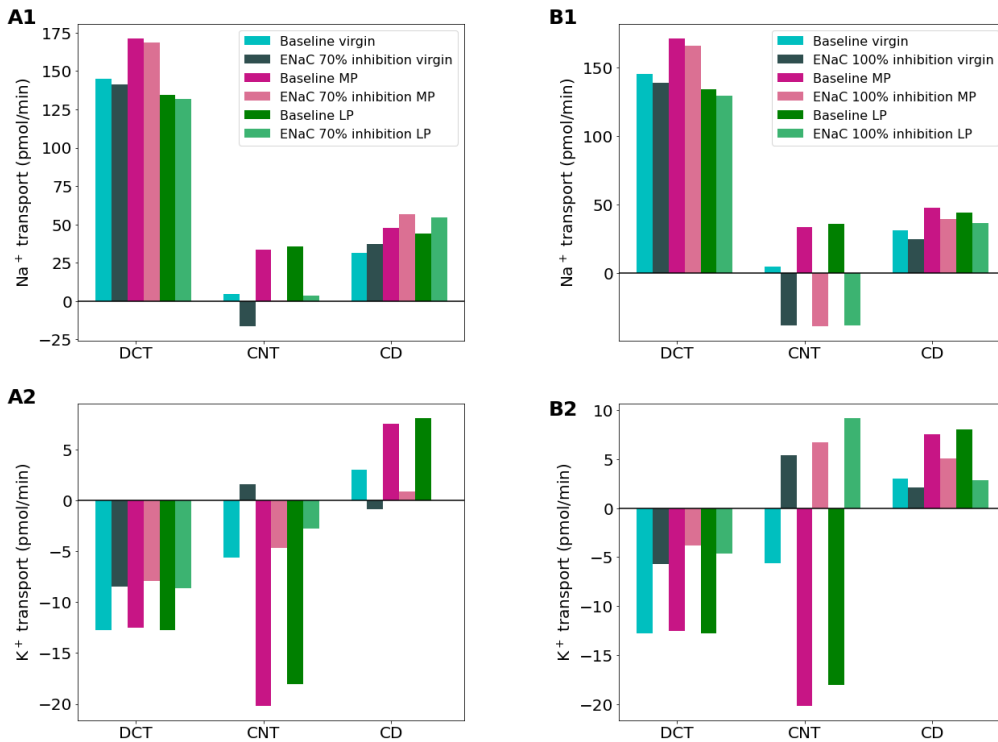


FIGURE 4. Impact of epithelial Na^+ channel (ENaC) inhibition (panels A1 & A2, 70%; B1 & B2, 100%) on distal segment net segmental transport of Na^+ (A1 & B1) and K^+ (A2 & B2) along individual nephron segments in the virgin, mid-pregnant (MP), and late pregnant (LP) models. Notations are analogous to **Error! Reference source not found.**. Only the distal segments are shown because ENaC inhibition only affects distal segments.

West et al. [9] conducted experiments to test the effect of inhibition of the ENaC on

pregnancy and found that a chronic ENaC blockade ablated the normal pregnancy Na^+ retention. We conducted simulations to test the impact of a 70% ENaC inhibition and a full ENaC knockout (i.e., 100% inhibition) on our model predictions. Results are shown in Fig. 4.

When the ENaC is inhibited by 70%, there is a 19% reduction in Na^+ reabsorption along the DCT and CNT. Collecting duct Na^+ reabsorption does increase, but this loss results in a 48% increase in urinary Na^+ excretion. Similar effects are found in the MP and LP models with ENaC inhibition. In the LP model, there is a 21% decrease in Na^+ reabsorption along the DCT and CNT resulting in a 38% increase in urinary Na^+ excretion from baseline LP model results (Fig. 4A1). ENaC inhibition has an opposite effect on K^+ . Specifically, K^+ secretion is decreased by ENaC inhibition so much so that the models predict a net K^+ reabsorption along the CNT for each of the virgin, MP, and LP models. This significant change results in a net reduction in K^+ secretion along the distal segments of 82% in the MP model. In the end urinary excretion of K^+ is reduced by about 26% when compared to the baseline MP and LP models (Fig. 4B1).

A full ENaC knockout leads to even more drastic effects on Na^+ and K^+ handling in each of the virgin, MP, and LP model predictions when compared to 70% inhibition. Specifically, the CNT has net secretion of Na^+ with net reabsorption of K^+ . This happens likely because the ENaC is the primary Na^+ transporter along this segment. As a result, urinary Na^+ excretion is predicted to more than double while urinary K^+ excretion is about 25% of baseline for the virgin, MP, and LP models (Figs. 4A2 and 4B2).

3.3 Effect of H^+ - K^+ -ATPase knockout on Na^+ and K^+ transport

Walter et al. [10] conducted experiments to test the effect of H^+ - K^+ -ATPase knockout (HKA-KO) on Na^+ and K^+ regulation in pregnant mice and found that pregnant HKA-KO mice had only a modestly expanded plasma volume and altered K^+ balance when compared to pregnant wild-type mice.

We conducted two types of HKA-KO experiments. In the first simulation we did a full 100% inhibition of the H^+ - K^+ -ATPase transporter only. We will refer to this simulation as HKA-KO. In the second simulation we also added a change in the Na^+ - Cl^- cotransporter, ENaC, and Pendrin transporters as observed in Walter et al. [10]. We will refer to this simulation as HKA-KO-preg. Results are shown in Fig. 5.

Net K^+ secretion along the DCT and CNT is predicted to increase by 85% and 77% in the MP HKA-KO and LP HKA-KO simulations, respectively, when compared to the baseline MP and LP models. This results in about a 60% increase in urinary K^+ excretion for both pregnant HKA-KO models. The virgin HKA-KO model does have an increase in K^+ secretion along these segments, but by a smaller fraction of 34%, yielding a 41% increase in urinary K^+ excretion when compared to the baseline virgin model. Na^+ handling is slightly altered, but results in only a 5% increase in urinary Na^+ excretion for each of the virgin, MP, and LP model simulations.

Walter et al. (44) found that in pregnant H^+ - K^+ -ATPase type 2 knockout mice, the Na^+ - Cl^- cotransporter, ENaC, and Pendrin transporter were altered as well from normal pregnancy adaptations. We added these changes to the HKA-KO study to get the HKA-KO-preg simulations to see how results may be altered by these other adaptations. These adaptations alter how Na^+ and K^+ is handled along the distal segments when compared to only the HKA-

KO in isolation. Specifically, in the HKA-KO-preg MP simulations, K^+ secretion along the DCT and CNT is 32% higher than baseline MP simulations. Similarly, the HKA-KO-preg LP simulation has a 19% increase in K^+ secretion along these segments when compared to baseline. This is likely due to the decreased ENaC activity that normally increases K^+ secretion in these segments. In the end urinary K^+ excretion for the HKA-KO-preg MP and LP simulations is 42% higher than the respective baseline MP and LP model predictions. Additionally, since there is Na^+ transporter changes, Na^+ handling is altered such that urinary Na^+ excretion is increased by about 24% in both the HKA-KO-preg MP and LP models when compared to the respective baseline model predictions.

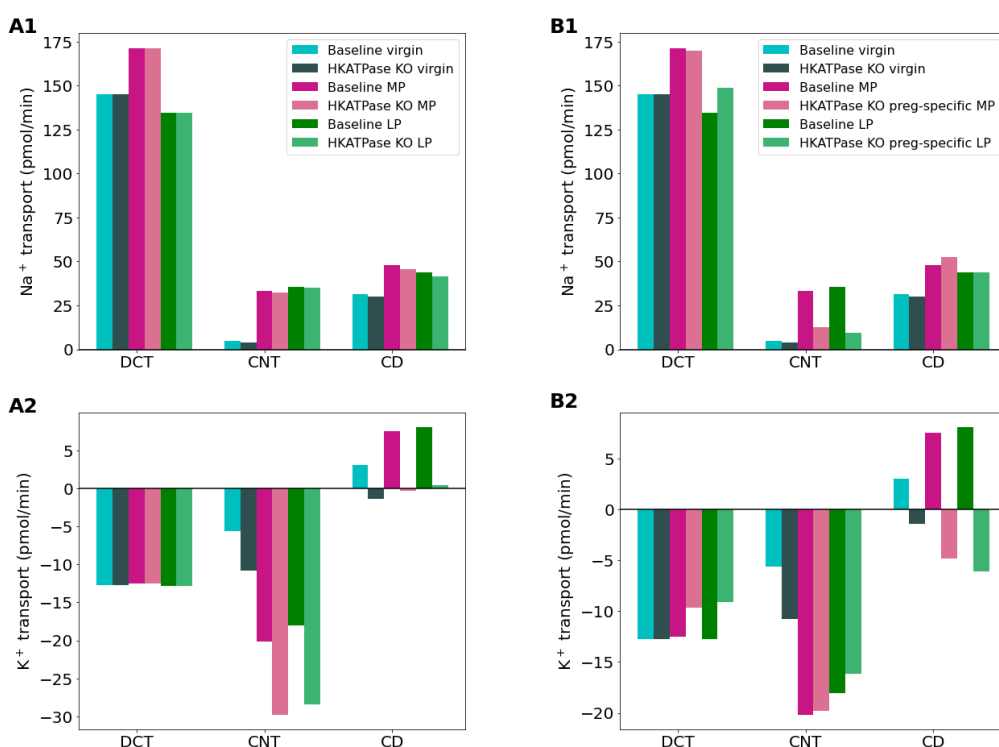


FIGURE 5. Impact of H^+K^+ -ATPase knockout (KO) study on distal segment net segmental transport of Na^+ (A1 & B1) and K^+ (A2 & B2) along individual nephron segments in the virgin, mid-pregnant (MP), and late pregnant (LP) models. Left panels show results for clean KO. For the right panels, pregnancy models also include changes to the pregnancy-specific renal adaptations of the Na^+Cl^- cotransporter, epithelial Na^+ channel, and $Cl^-HCO_3^-$ exchanger. Notations are analogous to **Error! Reference source not found.** Only the distal segments are shown because H^+K^+ -ATPase inhibition only affects distal segments.

4 DISCUSSION

Pregnancy induces major changes in the structure and function of the kidney, resulting in kidney growth as well as elevated blood flow, in a process that changes continually throughout pregnancy [1]. A particular drastic change is the $\sim 30\%$ increase in GFR in pregnant rats [3]. Although osmolality of the plasma is slightly decreased, this increase in GFR results in an increased filtered load to the nephrons during pregnancy. How do the nephrons of a pregnant rat handle the increased filtered load? Pregnancy-induced renal

adaptations, as recently reviewed by de Souza and West [2], are complex and extensive. How might those coordinated changes not only meet that increased demand but retain electrolytes? These are the questions that the present study sought to answer.

The increase in plasma volume required to supply the developing fetus and placenta is largely driven by Na^+ retention. About half of that Na^+ transport takes place along the proximal tubules and is mediated by the NHE3, which is upregulated in pregnancy. Our previous analysis [11] has indicated that in the absence of this adaptation, the water and electrolyte retention required in pregnancy would not have been possible. Downstream of the proximal tubules, the distal tubular segments are responsible for fine tuning the remaining filtrate so that urinary excretion approximates equal intake. West et al. [9] found that chronic ENaC blockade in pregnant rats resulted in significantly reduced Na^+ retention and plasma volume expansion and pups with a lower birth weight. Model analysis also demonstrated the importance of massively increased ENaC activity during pregnancy.

One key limitation is that the present models represent only a superficial nephron, whereas one-third of the nephrons are juxtamedullary nephrons that reach into the inner medulla. Also, the models assume that the interstitial fluid composition is known a priori. There are changes in these models that may affect interstitial fluid composition, but since there is no evidence that has measured these changes, we did not include those changes in our model assumptions. Interactions among nephron segments and the renal vasculature can be modelled using the approaches in Refs. [30-43].

This study focused on renal adaptations in a normal pregnancy, which is characterized by avid plasma volume expansion as well as Na^+ and K^+ retention. In a NP state, hypertension is generally associated with water and Na^+ retention. Interestingly, that association appears to be broken during pregnancy. Remarkably, pregnancy tends to have an antihypertensive effect on spontaneously hypertensive rats [27]. Hypertension during pregnancy is highly complicated and not fully understood. In addition, hypertensive disorders of pregnancy (meaning the onset of high blood pressure after start of gestation), such as gestational hypertension or preeclampsia, are associated with a lower plasma volume than normal pregnancy [1]. Further complicating the picture is the observation that hypertension alters renal transport differently in virgin and pregnant rats. Abreu et al. [44] showed that in a virgin hypertensive rat, NHE3 and NCC are upregulated significantly and NKCC2 is slightly downregulated leading to increased Na^+ reabsorption compared with normotensive virgin control. However, in a MP hypertensive rat, Na^+ transporter NHE3 mRNA expression was significantly downregulated compared with normotensive MP rat control [44]. How do these hypertension-induced renal transport changes affect kidney function differently in NP and pregnancy? A combination of experimental, clinical, and theoretical efforts may be required to fully understand the pathogenesis of hypertension in pregnancy, including preeclampsia. Theoretical efforts may leverage the sex-specific computational models that have been developed for blood pressure regulation [45-51].

REFERENCES

- [1] C. A. West, J. M. Sasser, and C. Baylis, "The enigma of continual plasma volume expansion in pregnancy: critical role of the renin-angiotensin-aldosterone system," *American Journal of Physiology-Renal Physiology*, vol. 311, no. 6, pp. F1125-F1134, 2016.

- [2] A. M. de Souza and C. A. West, "Adaptive remodeling of renal Na⁺ and K⁺ transport during pregnancy," *Current Opinion in Nephrology and Hypertension*, vol. 27, no. 5, pp. 379-383, 2018.
- [3] C. Baylis, "Renal hemodynamics and volume control during pregnancy in the rat," in *Seminars in nephrology*, 1984, vol. 4, no. 3: Elsevier, pp. 208-220.
- [4] J. Atherton and S. C. Pirie, "The effect of pregnancy on glomerular filtration rate and salt and water reabsorption in the rat," *The Journal of Physiology*, vol. 319, no. 1, pp. 153-164, 1981.
- [5] C. West, Z. Zhang, G. Ecker, and S. M. Masilamani, "Increased renal α -epithelial sodium channel (ENAC) protein and increased ENAC activity in normal pregnancy," *American Journal of Physiology-Regulatory, Integrative and Comparative Physiology*, vol. 299, no. 5, pp. R1326-R1332, 2010.
- [6] J. Mahaney, C. Felton, D. Taylor, W. Fleming, J. Kong, and C. Baylis, "Renal cortical Na⁺-K⁺-ATPase activity and abundance is decreased in normal pregnant rats," *American Journal of Physiology-Renal Physiology*, vol. 275, no. 5, pp. F812-F817, 1998.
- [7] C. A. West, S. D. Beck, and S. M. Masilamani, "Time course of renal sodium transport in the pregnant rat," *Current Research in Physiology*, vol. 4, pp. 229-234, 2021.
- [8] R. Hu, A. A. McDonough, and A. T. Layton, "Sex-Differences in Solute Transport Along the Nephrons: Effects of Na⁺ Transport Inhibition," *American Journal of Physiology-Renal Physiology*, 2020.
- [9] C. A. West, W. Han, N. Li, and S. M. Masilamani, "Renal epithelial sodium channel is critical for blood pressure maintenance and sodium balance in the normal late pregnant rat," *Experimental physiology*, vol. 99, no. 5, pp. 816-823, 2014.
- [10] C. Walter, C. Rafael, S. Lasaad, S. Baron, A. Salhi, and G. Crambert, "H, K-ATPase type 2 regulates gestational extracellular compartment expansion and blood pressure in mice," *American Journal of Physiology-Regulatory, Integrative and Comparative Physiology*, vol. 318, no. 2, pp. R320-R328, 2020.
- [11] M. M. Stadt and A. T. Layton, "Adaptive changes in single-nephron GFR, tubular morphology, and transport in a pregnant rat nephron: modeling and analysis," *American Journal of Physiology-Renal Physiology*, vol. 322, no. 2, pp. F121-F137, 2022.
- [12] A. T. Layton, V. Vallon, and A. Edwards, "Adaptive Changes in GFR, Tubular Morphology and Transport in Subtotal Nephrectomized Kidneys: Modeling and Analysis," *Am J Physiol Renal Physiol*, vol. 313, no. 2, pp. F199-F209, 2017.
- [13] A. T. Layton, V. Vallon, and A. Edwards, "A computational model for simulating solute transport and oxygen consumption along the nephrons," *Am J Physiol Renal Physiol*, vol. 311, no. 6, pp. F1378-F1390, Dec 1 2016, doi: 10.1152/ajprenal.00293.2016.
- [14] A. Edwards, H. Castrop, K. Laghmani, V. Vallon, and A. T. Layton, "Effects of NKCC2 isoform regulation on NaCl transport in thick ascending limb and macula densa: a modeling study," *Am J Physiol Renal Physiol*, vol. 307, no. 2, pp. F137-46, Jul 15 2014, doi: 10.1152/ajprenal.00158.2014.
- [15] A. T. Layton, V. Vallon, and A. Edwards, "Modeling oxygen consumption in the proximal tubule: effects of NHE and SGLT2 inhibition," *Am J Physiol Renal Physiol*, vol. 308, no. 12, pp. F1343-57, Jun 15 2015, doi: 10.1152/ajprenal.00007.2015.
- [16] A. T. Layton, V. Vallon, and A. Edwards, "Predicted consequences of diabetes and SGLT inhibition on transport and oxygen consumption along a rat nephron," *Am J Physiol Renal Physiol*, vol. 310, no. 11, pp. F1269-83, Jun 1 2016, doi: 10.1152/ajprenal.00543.2015.
- [17] A. T. Layton, A. Edwards, and V. Vallon, "Renal potassium handling in rats with subtotal nephrectomy: Modeling and Analysis," *Am J Physiol Renal Physiol*, 2017.

- [18] A. T. Layton and V. Vallon, "SGLT2 Inhibition in a Kidney with Reduced Nephron Number: Modeling and Analysis of Solute Transport and Metabolism," *Am J Physiol Renal Physiol*, vol. 314, no. 5, pp. F969-F984, Jan 17 2018, doi: 10.1152/ajprenal.00551.2017.
- [19] A. T. Layton, K. Laghmani, V. Vallon, and A. Edwards, "Solute transport and oxygen consumption along the nephrons: effects of Na⁺ transport inhibitors," *Am J Physiol Renal Physiol*, vol. 311, no. 6, pp. F1217-F1229, Dec 1 2016, doi: 10.1152/ajprenal.00294.2016.
- [20] R. Hu, A. A. McDonough, and A. T. Layton, "Functional implications of the sex differences in transporter abundance along the rat nephron: modeling and analysis," *Am J Physiol Renal Physiol*, vol. 317, no. 6, pp. F1462-F1474, Dec 1 2019, doi: 10.1152/ajprenal.00352.2019.
- [21] R. Hu, A. A. McDonough, and A. T. Layton, "Sex differences in solute and water handling in the human kidney: Modeling and functional implications," *iScience*, 2021.
- [22] A. T. Layton and H. E. Layton, "A Computational Model of Epithelial Solute and Water Transport along a Human Nephron," *PLoS Comput Biol*, 2018.
- [23] R. Hu and A. T. Layton, "A Computational Model of Kidney Function in a Patient with Diabetes," *International journal of molecular sciences*, 2021.
- [24] C. A. West *et al.*, "Renal and colonic potassium transporters in the pregnant rat," *American Journal of Physiology-Renal Physiology*, vol. 314, no. 2, pp. F251-F259, 2018.
- [25] C. Baylis, "Renal effects of cyclooxygenase inhibition in the pregnant rat," *American Journal of Physiology-Renal Physiology*, vol. 253, no. 1, pp. F158-F163, 1987.
- [26] S. Churchi-I, H. H. Bengele, and E. A. Alexander, "Sodium balance during pregnancy in the rat," *American Journal of Physiology-Regulatory, Integrative and Comparative Physiology*, vol. 239, no. 1, pp. R143-R148, 1980.
- [27] J. Davison and M. Lindheimer, "Changes in renal haemodynamics and kidney weight during pregnancy in the unanaesthetized rat," *The Journal of physiology*, vol. 301, no. 1, pp. 129-136, 1980.
- [28] H. Garland, R. Green, and R. Moriarty, "Changes in body weight, kidney weight and proximal tubule length during pregnancy in the rat," *Kidney and Blood Pressure Research*, vol. 1, no. 1, pp. 42-47, 1978.
- [29] A. Odutayo and M. Hladunewich, "Obstetric nephrology: renal hemodynamic and metabolic physiology in normal pregnancy," *Clinical Journal of the American Society of Nephrology*, vol. 7, no. 12, pp. 2073-2080, 2012.
- [30] A. T. Layton and H. E. Layton, "Countercurrent multiplication may not explain the axial osmolality gradient in the outer medulla of the rat kidney," *Am J Physiol Renal Physiol*, vol. 301, no. 5, pp. F1047-F1056, 2011.
- [31] A. T. Layton, T. L. Pannabecker, W. H. Dantzler, and H. E. Layton, "Functional implications of the three-dimensional architecture of the rat renal inner medulla," *Am J Physiol Renal Physiol*, vol. 298, no. 4, pp. F973-87, Apr 2010, doi: 10.1152/ajprenal.00249.2009.
- [32] B. C. Fry, A. Edwards, and A. T. Layton, "Impact of nitric-oxide-mediated vasodilation and oxidative stress on renal medullary oxygenation: a modeling study," *Am J Physiol Renal Physiol*, vol. 310, no. 3, pp. F237-F247, 2016.
- [33] B. C. Fry, A. Edwards, I. Sgouralis, and A. T. Layton, "Impact of renal medullary three-dimensional architecture on oxygen transport," *Am J Physiol Renal Physiol*, vol. 307, no. 3, pp. F263-72, Aug 1 2014, doi: 10.1152/ajprenal.00149.2014.
- [34] B. C. Fry, A. Edwards, and A. T. Layton, "Impacts of nitric oxide and superoxide on renal medullary oxygen transport and urine concentration," *Am J Physiol Renal Physiol*, vol. 308, no. 9, pp. F967-80, May 1 2015, doi: 10.1152/ajprenal.00600.2014.
- [35] A. T. Layton, R. L. Gilbert, and T. L. Pannabecker, "Isolated interstitial nodal spaces may facilitate preferential solute and fluid mixing in the rat renal inner medulla," *Am J Physiol Renal Physiol*, vol. 302, no. 7, pp. F830-F839, 2012.

- [36] A. T. Layton, H. E. Layton, W. H. Dantzler, and T. L. Pannabecker, "The mammalian urine concentrating mechanism: hypotheses and uncertainties," *Physiology (Bethesda)*, vol. 24, pp. 250-6, Aug 2009, doi: 10.1152/physiol.00013.2009.
- [37] J. Chen, A. T. Layton, and A. Edwards, "A mathematical model of O₂ transport in the rat outer medulla. I. Model formulation and baseline results," *Am J Physiol Renal Physiol*, vol. 297, no. 2, pp. F517-36, Aug 2009, doi: 10.1152/ajprenal.90496.2008.
- [38] J. Chen, A. Edwards, and A. T. Layton, "A mathematical model of O₂ transport in the rat outer medulla. II. Impact of outer medullary architecture," *Am J Physiol Renal Physiol*, vol. 297, no. 2, pp. F537-48, Aug 2009, doi: 10.1152/ajprenal.90497.2008.
- [39] J. Chen, I. Sgouralis, L. C. Moore, H. E. Layton, and A. T. Layton, "A mathematical model of the myogenic response to systolic pressure in the afferent arteriole," *Am J Physiol Renal Physiol*, vol. 300, no. 3, pp. F669-81, Mar 2011, doi: 10.1152/ajprenal.00382.2010.
- [40] A. T. Layton, "A mathematical model of the urine concentrating mechanism in the rat renal medulla. I. Formulation and base-case results," *Am J Physiol Renal Physiol*, vol. 300, no. 2, pp. F356-71, Feb 2011, doi: 10.1152/ajprenal.00203.2010.
- [41] A. T. Layton, "A mathematical model of the urine concentrating mechanism in the rat renal medulla. II. Functional implications of three-dimensional architecture," *Am J Physiol Renal Physiol*, vol. 300, no. 2, pp. F372-84, Feb 2011, doi: 10.1152/ajprenal.00204.2010.
- [42] A. T. Layton, W. H. Dantzler, and T. L. Pannabecker, "Urine concentrating mechanism: impact of vascular and tubular architecture and a proposed descending limb urea-Na⁺ cotransporter," *Am J Physiol Renal Physiol*, vol. 302, no. 5, pp. F591-605, Mar 1 2012, doi: 10.1152/ajprenal.00263.2011.
- [43] A. T. Layton and H. E. Layton, "A region-based model framework for the rat urine concentrating mechanism," *Bull Math Biol*, vol. 65, no. 5, pp. 859-901, Sep 2003, doi: 10.1016/S0092-8240(03)00045-4.
- [44] A. NP, J. C. B. M. Tardin, M. A. Boim, R. R. Campos, C. T. Bergamaschi, and N. Schor, "Hemodynamic parameters during normal and hypertensive pregnancy in rats: evaluation of renal salt and water transporters," *Hypertension in pregnancy*, vol. 27, no. 1, pp. 49-63, 2008.
- [45] A. T. Layton, "His and Her Mathematical Models," *CAIMS Blog*, 2020.
- [46] S. Ahmed, R. Hu, J. Leete, and A. T. Layton, "Understanding sex differences in long-term blood pressure regulation: insights from experimental studies and computational modeling," *American Journal of Physiology-Heart and Circulatory Physiology*, vol. 316, no. 5, pp. H1113-H1123, 2019.
- [47] S. Ahmed and A. T. Layton, "Sex-specific computational models for blood pressure regulation in the rat," *Am J Physiol Renal Physiol*, 2019.
- [48] S. Ahmed, J. C. Sullivan, and A. T. Layton, "Impact of sex and pathophysiology on optimal drug choice in hypertensive rats: quantitative insights for precision medicine," *Iscience*, vol. 24, no. 4, p. 102341, 2021.
- [49] J. G. Leete, S; Layton, AT, "Modeling Sex Differences in the Renin Angiotensin System and the Efficacy of Antihypertensive Therapies," *Computers & Chemical Engineering*, vol. 112, pp. 253-264, 2018.
- [50] J. Leete and A. T. Layton, "Sex-specific long-term blood pressure regulation: Modeling and analysis," *Comput Biol Med*, vol. 104, pp. 139-148, Jan 2019, doi: 10.1016/j.combiomed.2018.11.002.
- [51] S. Abo, D. Smith, M. Stadt, and A. Layton, "Modelling female physiology from head to Toe: Impact of sex hormones, menstrual cycle, and pregnancy," *Journal of Theoretical Biology*, p. 111074, 2022.